Waxy-Crude Production Management in a Deepwater Subsea Environment

S. Suppiah, SPE, **A. Ahmad,** SPE, and **C. Alderson,** SPE, Murphy Oil; and **K. Akbarzadeh,** SPE, **J. Gao,** SPE, **J. Shorthouse,** SPE, **I.A. Khan,** SPE, **C. Forde,** SPE, and **A. Jamaluddin,** SPE, Schlumberger

Summary

Systematic experimental and modeling approaches to designing a safe operating strategy for a 5-km deepwater-subsea-flowline case study are presented to address unplanned shutdown and restart events for waxy-crude production. The measurements confirmed that the fluid behaves like Bingham plastic when it is allowed to become gel at the seabed temperature of 4°C. The cool-down period was modeled using the transient simulator validated by measurements and was predicted to take 21 hours. The restart pressure was then modeled for both stock-tank and at-line pressure conditions. These restart pressure requirements were found to be 2,500 and 2,100 psi, respectively, for stock-tank and at-line pressure conditions. Also, the use of pour-point depressants demonstrated that the fluid would not form gel at the seabed temperature of 4°C. However, the current shut-in wellhead pressure of 2,500 psi is deemed adequate to restart the lines in the event of unplanned shutdown without the use of chemicals. The presence of a subsea pig-launching pump provides a safety factor for restart in case the line pressure is released to atmospheric conditions. Hence, the operating strategy does not require injection of pour-point depressants at the current state. However, in future when the shut-in wellhead pressure falls below 2,500 psi, the operating strategy is expected to be modified accordingly.

Introduction

Development activities in the deepwater and frontier arena face significant challenges. The colder seabed temperatures and larger pressure drops caused by longer tieback lines connecting subsea trees to a production facility are of particular concern. In addition, because of the high cost of deepwater wells, fluids from different reservoirs and fields are commingled and produced through long subsea lines, enhancing the potential for fluid incompatibility. Fluid phase behavior, fluid flow, heat transfer, and precipitation and deposition of hydrocarbon solids such as waxes and asphaltenes are key risk factors influencing safe operating strategies.

In most production systems, the inside-wall temperature is lower than the temperature of bulk fluid in the line. When the fluid temperature falls below its wax-appearance temperature (WAT), wax crystals appear in the system. These wax crystals are typically defined as the normal paraffins ranging from C_{18} to C_{60}. Precipitation of wax crystals in fluid has an impact on the rheological behavior of the oil. Crude-oil rheological properties demonstrate three distinct phases with cooling (Barry, 1971; Wardhaugh et al. 1988), and these phases are

- Newtonian behavior at a temperature above the WAT
- Power-law behavior at a temperature below the WAT
- Viscoplastic behavior at a temperature below the pour-point temperature of the fluid

The viscosity of waxy oil below its WAT depends not only on temperature but also on shear. If the fluid temperature is low enough, the precipitated wax crystals may create a wax network, which would result in gelation of oil if unplanned shutdown happens (Misra et al. 1971). During such events, restarting the system may cause operational problems. Therefore, it is of great importance to understand waxy-crude properties (Vinay et al. 2009), and consequently, develop a contingency plan along with the operating strategy for unplanned shutdown and restart events.

Experimental measurements as well as simulations can help in understanding the behavior of waxy crudes and the flow-assurance issues they may create. A set of flow-assurance measurements that can be performed for waxy crudes includes wax content, WAT, pour point, gel strength (GS), and deposition rates. Measured data from flow-assurance laboratory studies are typically used in simulation studies to predict the severity of probable flow-assurance issues for a variety of production-system configurations. Without proper calibration to representative experimental data, simulation studies may result in either overdesign or underdesign. An optimized design using representative experimental data would maximize value and could potentially identify opportunities in marginal fields that were assumed to be too costly to produce on the basis of conservative simulations.

In this paper, systematic experimental and modeling approaches to designing a safe operating strategy are presented to address unplanned shutdown and restart events for waxy-crude production. A case study for a 5-km deepwater (1200–1500 m) subsea flowline located in the South China Sea is discussed. A schematic of the field layout is presented in **Fig 1.** The wells and flowline pressure and temperature characteristics are presented in **Tables 1 through 3.** The fluid under study contained 11 wt% (%, w/w) wax with a WAT of 20°C at line-pressure conditions and approximately 25°C at stock-tank-oil (STO) condition. This difference is a result of solution gas at line-pressure conditions and is in line with what has been presented in literature (Ekweribe et al. 2008). Laboratory gel-strength and rheological properties were measured at both stock-tank and line-pressure conditions to obtain input parameters for subsequent transient simulation of shutdown and restart scenarios. Experiments were also conducted to evaluate the effectiveness of a commercial wax inhibitor.

In summary, this work demonstrates the following key aspects of designing operating strategies to reduce the risk related to production assurance in deepwater subsea developments and also optimize operating expenses:

1. The importance of experimental validations for any simulation work.
2. Influence of solution gas in waxy-crude properties such as WATs, gel-strength, and rheological properties.
3. A protocol to scale up the laboratory data to a practical field environment.
4. Strategies to optimize operating expenses with sufficient safety factors by modeling the total system.

Background Information

A systematic workflow was required for an independent evaluation of whether the flowline needed a continuous injection of chemicals to prevent gel in the flowline if an unplanned shutdown occurs. A simulation effort was undertaken to evaluate an operating strategy including a shutdown, prolonged downtime, and a restart using a commercial transient simulation package (OLGA^R). Simulation input parameters such as fluid composition, cloud point, or WAT, as well as rheological properties and GS of the fluids, were measured in the laboratory.

It has been demonstrated in literature that the critical wax properties (such as WAT, pour point, and rheology) are sufficiently lower with solution gas in the fluid system compared to a

Copyright © 2012 Society of Petroleum Engineers

This paper (SPE 132615) was accepted for presentation at the SPE Annual Technical Conference and Exhibition, Florence, Italy, 20–22 September 2010, and revised for publication. Original manuscript received for review 28 June 2010. Revised manuscript received for review 18 November 2010. Paper peer approved 24 January 2011.

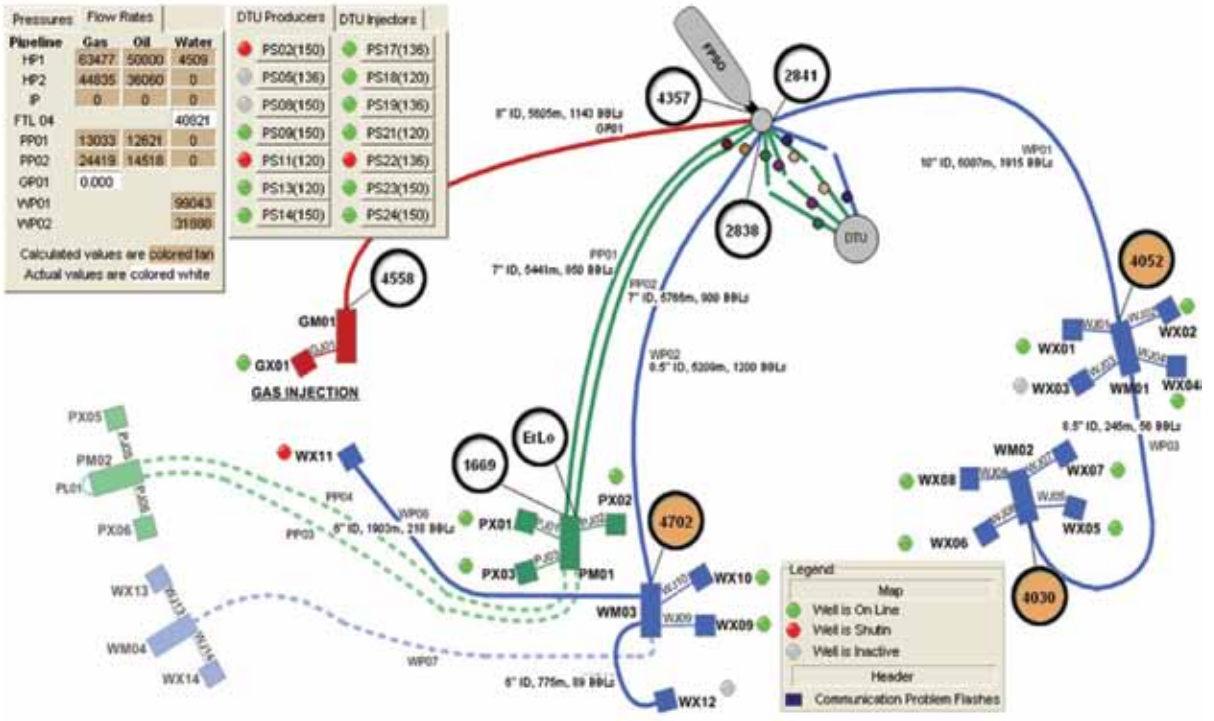

Fig. 1—Schematic of field layout.

TABLE 1—FIELD PARAMETERS

Parameters	Subsea wells		
	X1	X2	X3
Reservoir pressure, psi	4,945	4,332	5,030
Flowing BHT, °C (°F)	83.9 (183)	75.5 (168)	90.0 (194)
Bubblepoint pressure, psi/temperature, °F	4,764/181	3,602/169.5	-
GOR scf/stb (29 June 2008)	1,446	996	1,043
Subsea wellhead flowing T/P (°C/°F/psi)	76/168/2,807	68/155/2,115	68/155/2,135

depressurized flowline at STO conditions. Laboratory measurements were conducted for both STO and pressure conditions and used in the simulation. Our goal was to evaluate the option to keep the flowline under pressure conditions to take advantage of solution gas and avoid injection of continuous chemicals, influencing the operating cost of the flowlines. A systematic workflow adapted for this study is illustrated in **Fig. 2.**

Experimental Equipment and Procedure

Crude-Oil Sample. A waxy-crude-oil sample from Well "X2" from Field A located in the Southeast China Sea was evaluated in this study. The received separator oil sample was initially equilibrated at separator conditions of pressure and temperature under continuous rocking for 24 hours. This process would help the precipitated wax and/or potentially agglomerated asphaltenes, if any, dissolve and/or disperse back into the solution. To prepare a live-oil sample representative of bottomhole fluid, a separator gas sample was recombined with the separator oil sample in such a way that the recombined reservoir fluid had the gas/oil ratio (GOR) of the bottomhole fluid. The recombined reservoir fluid was then conditioned before compositional analysis.

TABLE 2—FLUID CHARACTERISTICS

Parameters	Values
Wax content, % (w/w)	11.0
STO cloud point–WAT, °C (°F)	24 (75)–26 (79)
Pour point, °C (°F)	18 (64)–23 (73)
Seabed T, °C (°F)	4 (39)

Compositional Analysis. To ensure that the prepared recombined fluid was representative of the bottomhole fluid, C_{30}^{+} composition and GOR of the recombined fluid were determined. For this purpose, an accurately measured volume of the conditioned single-phase fluid was isobarically displaced into a pycnometer in which its density and mass were evaluated. The pycnometer was then connected to a GOR single-stage flash apparatus in which the oil was flashed to ambient pressure and temperature conditions. Next, the evolved gas phase was circulated through the residual liquid for a period of time to achieve equilibrium between the phases. Following circulation, the volume of equilibrium vapor and the mass of liquid remaining in the pycnometer were measured. The vapor phase was analyzed to C_{15+} with gas chromatography (GC), while the residual liquid was analyzed to C_{30+} with GC. From the measured composition and total mass of each phase, the composition of the original live oil was calculated using mass balance.

TABLE 3—FPSO-ARRIVAL TEMPERATURE AND PRESSURE		
Parameters	Flowline 1	Flowline 2
Floating production, storage, and offloading vessel (FPSO) arrival T, °C (°F)	45 (113)	45 (114)
FPSO arrival P, psi	607	620

A sample of STO was also prepared and analyzed using a high-temperature gas chromatography (HTGC) to measure the *n*-alkane wax content of the oil. These data can be entered into thermodynamic models that can predict WAT values closer to the measured values than those using the wax content obtained by other methods such as bulk filtration at low temperatures.

WAT. The WAT of the STO was measured using the cross-polar microscopy (CPM) technique (Karan et al. 2000). A subsample of the conditioned STO sample was placed on the CPM hot stage at 60°C. The sample was then cooled with a cooling rate of 0.5°C/min. During cooling, the intensity of the polarized light and photomicrographs of the CPM were recorded. The WAT was then determined from the abrupt change in the slope of the polarized-light power and was compared with the WATs determined from the images. The reported values are accurate to 0.5°C.

To determine the WAT of the live fluid, the conditioned fluid inside the pressure/volume/temperature (PVT) cell was cooled isobarically and monitored for wax precipitation through high-pressure CPM (HPCPM) and with the solid-detection system (SDS) (Karan et al. 2000). During cooling, the power of the transmitted light (PTL) and photomicrographs of the sample were recorded. The WAT was then determined from the change in the slope of the PTL and compared with the WAT determined from the HPCPM photomicrographs.

For the WAT measurements at pressures below the bubblepoint pressure of the fluid, the system was equilibrated at the test pressure and reservoir temperature for approximately 4 hours. The liquid phase was then measured for its WAT, as already explained.

GS. The GSs (or yield strength) of both STO and live recombined fluid were determined using model-pipeline-test (MPT) apparatus (Karan et al. 2000). The fluid was first placed in a test coil at 60°C and was subsequently cooled to 4°C, with a cooling rate of 5°C/hour. Next the cold fluid within the coil was aged statically for 8 hours. Then, the ungelling process took place by applying a pressure gradient using nitrogen. A more detailed description of the MPT can be found elsewhere (Karan et al. 2000).

Rheology. A high-pressure/high-temperature (HP/HT) concentric-cylinder rheometer was used for rheology studies. The HP/HT rheometer is rated to pressures up to 5,800 psia and for a temperature range of –10 to 200°C. The HP/HT rheometer consists of the rheometer drive unit and a high-pressure rheometry cell. Because of the intrinsic friction in the bearing, the minimum measured viscosity is approximately 20 mPa·s. Therefore, the measured viscosity values below 20 mPa·s are not reliable. Above the minimum measured viscosity of 20 mPa·s, the accuracy of the measurement is ± 10%. For STOs, the minimum measured viscosity is 5 mPa·s when using the open cup and bob arrangement. Hence, care should be taken when using the viscosity data measured below 20 mPa·s with the HP/HT rheometer.

Experimental Results and Discussion

Compositional Analysis. The detailed compositional analysis of the recombined fluid and a summary of its properties are presented in **Tables 4 and 5,** respectively. Measured GOR for the recombined fluid was 1,058 scf/STB. The measured bubblepoint of the recombined fluid at reservoir temperature of 76°C was 3,660 psia.

The *n*-alkane wax distribution of the STO sample measured by HTGC is presented in **Table 6.** The *n*-alkane wax content of the STO (C_{18+}) using HTGC was 11.2 wt%.

WAT. Fig. 3 demonstrates the detected WATs from both SDS plots and cross-polar microscopy for the live oil at two pressures as well as the STO. The measured WATs are shown in **Fig. 4.** As shown, there is approximately 7°C difference between the WAT measured for STO and that for the live-oil samples. The measured WATs for live fluid samples at 4,000 psi (above bubblepoint) and 2,200 psi (below bubblepoint) were approximately the same. The main reason could be the amount of gas still dissolved in the liquid phase at 2,200 psi (GOR of 569 scf/STB at 2,200 psi compared with 1,058

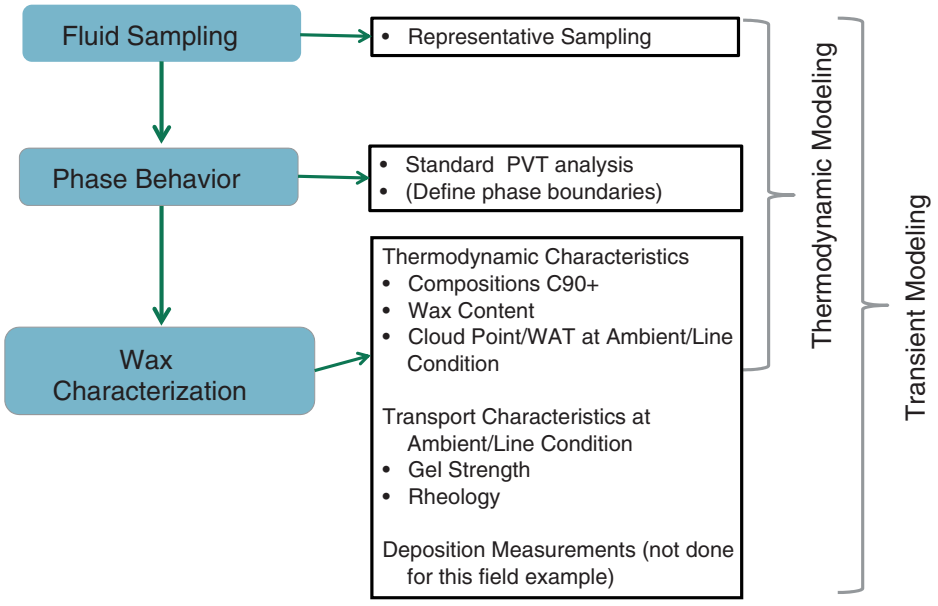

Fig. 2—A systematic workflow process. PVT is pressure/volume/temperature.

TABLE 4—C_{30+} COMPOSITIONAL ANALYSIS OF RECOMBINED RESERVOIR-FLUID SAMPLE

Component	MW	Flashed gas		Flashed oil		Monophasic	
	(g/mol)	(wt%)	(mol%)	(wt%)	(mol%)	(wt%)	(mol%)
CO_2	44.01	1.444	0.728	0.000	0.000	0.252	0.463
H_2S	34.08	0.000	0.000	0.000	0.000	0.000	0.000
N_2	28.01	0.175	0.139	0.000	0.000	0.031	0.088
C1	16.04	56.682	78.430	0.000	0.000	9.900	49.810
C2	30.07	11.396	8.413	0.000	0.000	1.991	5.343
C3	44.10	13.337	6.714	0.202	0.835	2.496	4.569
i-C4	58.12	5.651	1.173	0.110	0.344	0.627	0.870
n-C4	58.12	2.033	2.158	0.364	1.144	1.288	1.788
i-C5	72.15	1.665	0.625	0.430	1.088	0.710	0.794
n-C5	72.15	1.558	0.512	0.516	1.306	0.717	0.802
C6	84.00	0.503	0.412	1.513	3.288	1.521	1.461
Mcyclo-C5	84.16	0.106	0.133	0.818	1.775	0.763	0.732
Benzene	78.11	0.474	0.030	0.197	0.460	0.181	0.187
Cyclo-C6	84.16	0.529	0.125	1.059	2.297	0.957	0.918
C7	96.00	0.496	0.122	1.969	3.744	1.717	1.444
Mcyclo-C6	98.19	0.148	0.112	2.619	4.870	2.248	1.848
Toluene	92.14	0.277	0.036	1.014	2.008	0.863	0.756
C8	107.00	0.011	0.058	3.552	6.060	2.980	2.248
C2-Benzene	106.17	0.061	0.002	0.309	0.532	0.257	0.196
m & *p*-Xylene	106.17	0.017	0.013	1.355	2.330	1.129	0.858
o-Xylene	106.17	0.169	0.004	0.354	0.608	0.295	0.224
C9	121.00	0.130	0.031	2.740	4.134	2.291	1.528
C10	134.00	0.046	0.022	4.650	6.335	3.861	2.326
C11	147.00	0.016	0.007	3.950	4.905	3.268	1.794
C12	161.00	0.005	0.002	4.094	4.642	3.382	1.695
C13	175.00	0.002	0.001	5.026	5.243	4.149	1.913
C14	190.00	0.000	0.000	5.262	5.056	4.343	1.845
C15	206.00	0.000	0.000	6.849	6.070	5.653	2.215
C16	222.00	0.000	0.000	5.319	4.374	4.390	1.596
C17	237.00	0.000	0.000	4.852	3.737	4.004	1.364
C18	251.00	0.000	0.000	5.560	4.044	4.589	1.476
C19	263.00	0.000	0.000	4.279	2.970	3.531	1.084
C20	275.00	0.000	0.000	3.490	2.317	2.881	0.846
C21	291.00	0.000	0.000	3.226	2.024	2.663	0.739
C22	305.00	0.000	0.000	2.834	1.696	2.339	0.619
C23	318.00	0.000	0.000	2.572	1.477	2.123	0.539
C24	331.00	0.000	0.000	2.340	1.291	1.932	0.471
C25	345.00	0.000	0.000	2.211	1.170	1.825	0.427
C26	359.00	0.000	0.000	1.720	0.875	1.420	0.319
C27	374.00	0.000	0.000	1.811	0.884	1.494	0.323
C28	388.00	0.000	0.000	1.655	0.779	1.366	0.284
C29	402.00	0.000	0.000	1.592	0.723	1.314	0.264
C30+	539.81	0.000	0.000	7.589	2.567	6.263	0.937
Molecular weight (MW)			22.20		182.56		80.71
Mol%			63.51		36.49		

scf/STB at 4,000 psi). This difference could also be caused by the resolution of the SDS technique, which is unable to differentiate the size of the wax particles over this range of GORs.

GS. MPT apparatus was used to measure the GS of both STO and saturated live fluid at 2,200 psi. **Table 7** presents the results of these MPT tests. In the third GS test, the STO sample was treated with PPD at a concentration of 300 ppm and used for the study to investigate the impact of chemical inhibitor on the GS.

The cooling temperature profiles of STO, saturated live fluid at 2,200 psi, and treated STO in the MPT apparatus are shown in **Fig. 5.** After aging the oil for 8 hours, nitrogen was used to ungel the oil. Ungelling profiles (ΔP vs. time) for untreated STO and untreated live fluid are shown in **Fig. 6.** As shown, yield pressure (the pressure at which gel breaks) for the untreated STO and live fluid is 80.6 and 24.3 psi, respectively. For the treated STO, it was noticed that by adding more nitrogen both upstream and downstream pressures increased consistently, resulting in a constant ΔP.

TABLE 5—SUMMARY OF RECOMBINED-RESERVOIR-FLUID SAMPLE						
P_{res} (psia)	T_{res} (°C)	GOR (scf/stb)	°API	C_{30+} (wt%)	MW (g/mol)	Psat (psia)
4,332	76.4	1058	37.9	6.26	80.7	3,660

A constant ΔP was an indication of no gel formation at 4°C for the treated STO with 300 ppm of PPD.

The average yield stress τ_Y was calculated from the measured yield pressure P_Y by a simple force balance:

$$\tau_Y = \frac{P_Y D}{4L}, \quad (1)$$

where τ is shear pressure (Pa), P_Y is GS (Pa), D is pipeline diameter (m), and L is pipeline length (m). In these measurements, L is the coil length of 6.1 m and D is the coil inner diameter of 7.04 mm. The results of GS tests performed are summarized in Table 7.

It appears from these tests that the yield stress of the STO is the highest because of gel formation. The yield value becomes almost one-third by having solution gas in the system at a line pressure of 2,200 psia. These tests also demonstrate that treated oil prevents gelling of the waxy crude at a temperature of 4°C under a prolonged stagnant condition.

Rheology. The viscosity of the STO sample measured at 40°C as a function of shear rate is shown in **Fig. 7.** As shown in the plot, the oil viscosity did not change significantly with shear at this temperature which is above the detected STO WAT (i.e., 27°C). This means that the oil has a Newtonian behavior above its WAT.

Dependence of the measured viscosity of the STO sample at 4°C with changes in shear rate is shown in **Fig. 8.** The oil sample in the rheometer was first cooled from 60 to 27°C under dynamic conditions. Then, the cooling continued to 4°C under static conditions. At 4°C, the fluid was left for 8 hours to gel. Then a small shear rate was applied. Because there was no control over shear stress and the timesteps were not very small, the gel broke in less than 30 seconds. Therefore, the recorded data in this plot do not show the gel-breakage point and only show the shear-thinning effect; that is, the viscosity decreased by increasing shear rate at constant temperature.

Dependence of the measured viscosity of saturated live fluid at 2,200 psi and 4°C on shear rate is shown in the same plot (Fig. 8). The procedure for cooling the fluid from 60 to 4°C was similar to that explained for the STO sample. Again, the measured data points

TABLE 6—*n*-ALKANE PARAFFIN CARBON-NUMBER DISTRIBUTION OF STO SAMPLE FROM HTGC

Carbon number	*n*-Alkane concentration (wt%)	*n*-Alkane concentration (wt%)	Carbon number	*n*-Alkane concentration (ppm)	*n*-Alkane concentration (wt%)
18	15,289	1.529	50	12	0.001
19	11,652	1.165	51	13	0.001
20	10,525	1.053	52	11	0.001
21	9,953	0.995	53	12	0.001
22	9,289	0.929	54	10	0.001
23	8,880	0.888	55	11	0.001
24	8,164	0.816	56	10	0.001
25	7,482	0.748	57	11	0.001
26	6,333	0.633	58	11	0.001
27	5,644	0.564	59	11	0.001
28	4,529	0.453	60	9	0.001
29	3,941	0.394	61	9	0.001
30	2,790	0.279	62	7	0.001
31	2,584	0.258	63	8	0.001
32	1,422	0.142	64	5	0.001
33	1,207	0.121	65	6	0.001
34	563	0.056	66	4	0.000
35	614	0.061	67	5	0.000
36	134	0.013	68	0	0.000
37	105	0.011	69	0	0.000
38	61	0.006	70	0	0.000
39	46	0.005	71	0	0.000
40	35	0.003	72	0	0.000
41	29	0.003	73		
42	25	0.002	74		
43	22	0.002	75		
44	20	0.002	76		
45	20	0.002	77		
46	17	0.002	78		
47	17	0.002	79		
48	15	0.001	80		
49	14	0.001	81		
			Total	111,587	11.16

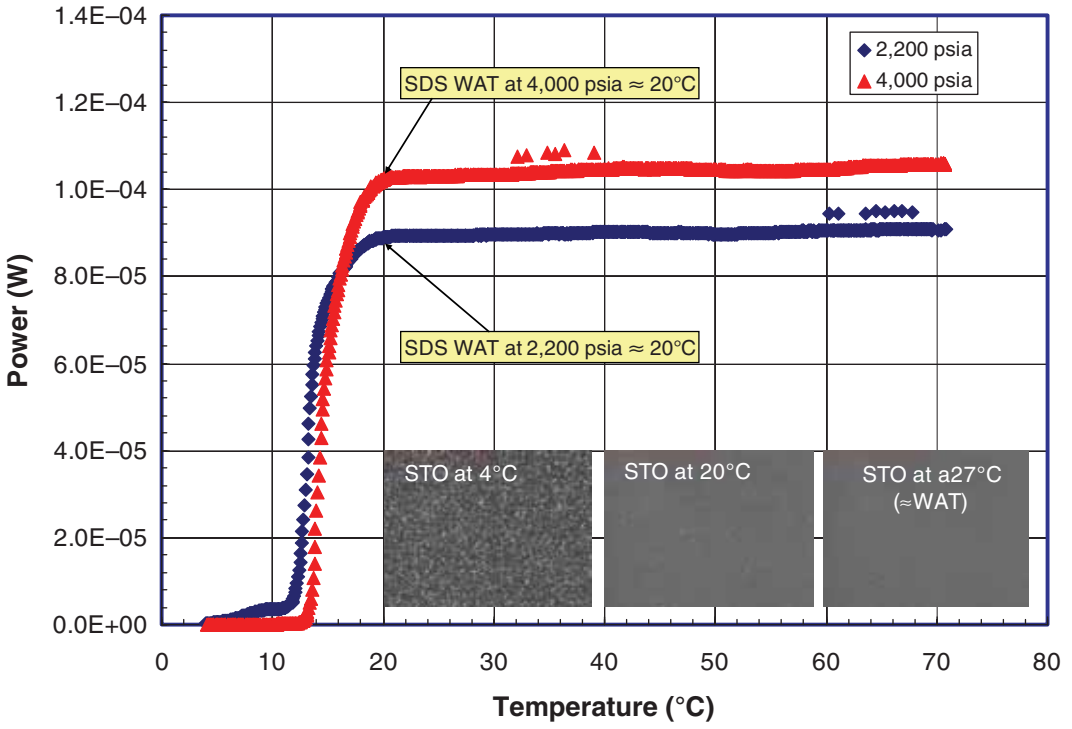

Fig. 3—Detected WATs for STO and live-oil samples.

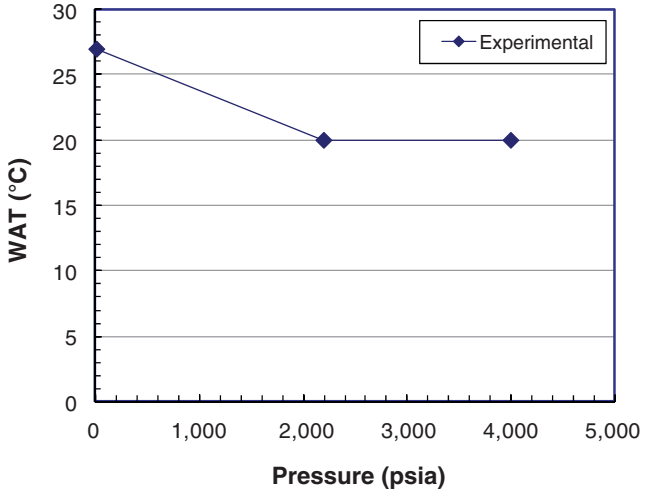

Fig. 4—Measured WATs vs. pressure.

show the viscosities after the gel-breaking point. As seen in Fig. 8, the live-oil viscosity data appear to behave in a fashion similar to that of the STO viscosities at similar shear rates because of the use of the logarithmic scale. However, there is a subtle difference in the values, as will be discussed later in the next section.

Transient Modeling of Shutdown and Restart Conditions

Background. A 7-in.-inside-diameter flexible line with an internal roughness of 0.7 mm has been considered as the modeling basis for both the flowline and riser sections. The flexible line has been built up in layers using the physical-properties data supplied in **Table 8. Table 9** summarizes soil properties used in this simulation. The flowline section is assumed to be half buried in soil that has the physical properties given in Table 6. Production was simulated using a fixed mass source of 12,000 B/D of dry liquid at 68.3°C.

The flowline and the riser used in the transient simulation of PP02 are schematically illustrated in **Fig. 9.** The minimum ambient seabed and the air temperatures are considered to be 4 and 20°C, respectively. The water-column temperatures are linearly interpolated between the minimum seabed and the ambient temperatures along the riser length. The maximum seawater current and the wind speed are assumed to be 0.5 and 5 m/s, respectively.

In this simulation study, wellhead temperature and pressure conditions are assumed to remain constant during the whole shutdown period. This simplified assumption is made owing to the fact that the wellhead pressure is below the bubblepoint pressure at the flowing wellhead temperature (Table 1). When the well is shut down, the well stream will segregate into a liquid column at the bottom of the wellbore and gas will accumulate at the wellhead. The wellhead pressure will be reduced as a result of cooling. However, the liquid column will be close to the reservoir temperature and, hence, unlikely to form gel. Hence, during restart, the wellhead is expected to reach flowing wellhead pressure reasonably quickly.

Fluid Phase Behavior. For thermodynamic simulation, the fluid composition presented in Table 4 has been used. The Soave-Redlich-Kwong (Soave 1972) equation of state with Péneloux (Péneloux et al. 1982) volume translation is used for the fluid modeling. Here the C_{7+} component is split into five pseudocomponents by use of an exponential distribution function. Pedersen's correlations

TABLE 7—RESULTS OF GS MEASUREMENTS

Test	Fluid type	Yield pressure, P_Y (psi)	Yield stress, τ_Y (Pa)
1	STO	80.6	160.3
2	Live oil at 2,200 psia	24.3	48.3
3	STO + 300 ppm PPD	---	No gel

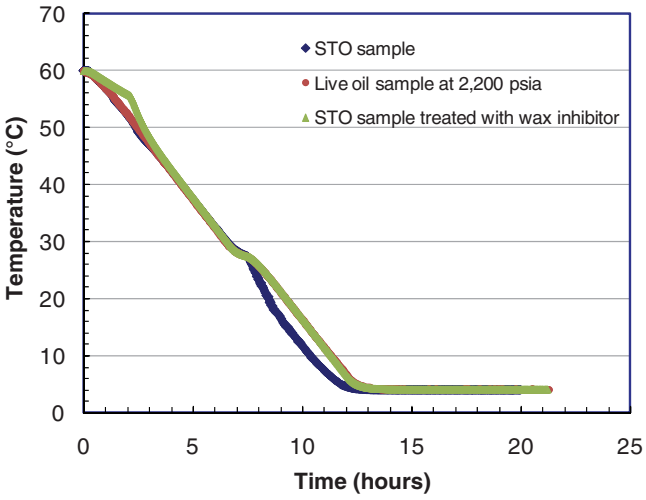

Fig. 5—Cooling profiles for samples in MPT apparatus.

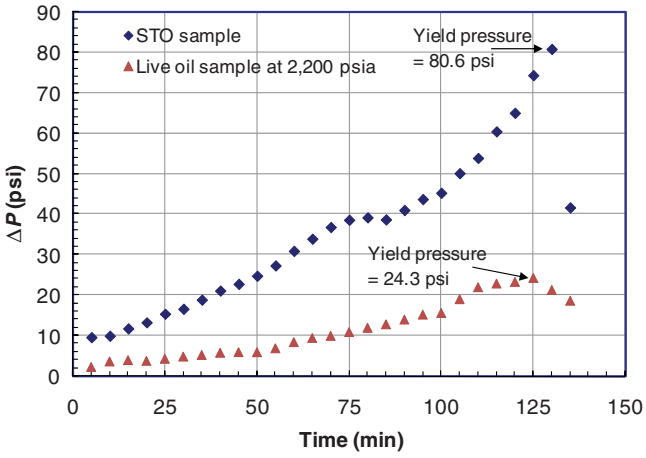

Fig. 6—Ungelling profiles and gel-breaking points for STO and live-oil samples.

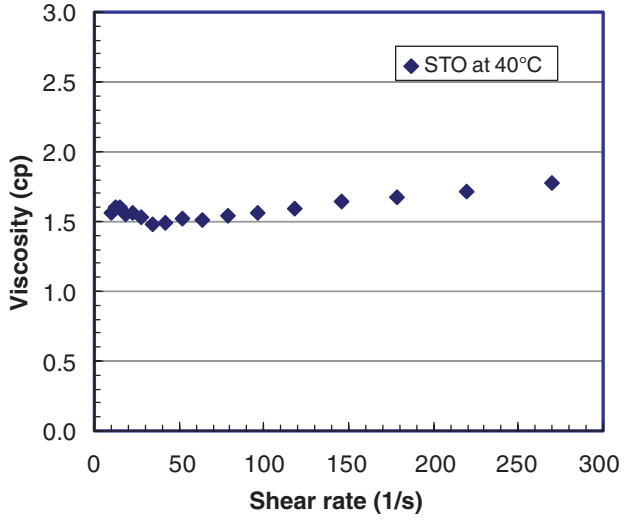

Fig. 7—Measured viscosities of STO sample at 40°C (shear-rate sweep).

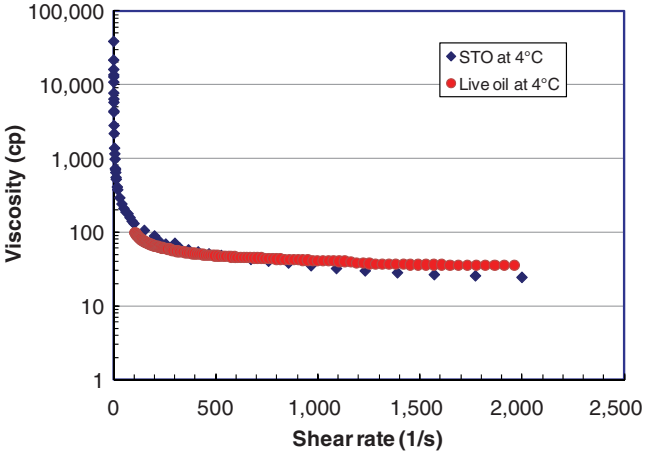

Fig. 8—Measured viscosities of STO sample at 4°C (shear-rate sweep).

TABLE 8—FLEXIBLE-LINE CONFIGURATION AND PROPERTIES

Material	Thickness (mm)	Heat Capacity (J/kg·K)	Conductivity (W/m·K)	Density (kg/m³)
SS	8.4	500	24.00	7900
PVDF	12.0	1200	2.40	1770
Carbon Steel	10.0	500	45.00	7830
PP	0.3	1925	0.14	900
Carbon Steel	03.0	500	45.00	7830
PP	0.6	1925	0.14	900
Glass Filament	0.8	500	45.00	7830
PP	0.6	1925	0.14	900
Carbon Steel	3.0	500	45.00	7830
PP	0.6	1925	0.14	900
Glass Filament	0.8	500	45.00	7830
PP	0.6	1925	0.14	900
PP Rubber	13.0	1925	0.14	900
PP Foam	22.0	1925	0.10	64
HDPE-Yellow	13.0	1900	0.40	966

TABLE 9—SOIL PROPERTIES			
Material	Heat Capacity (J/kg·K)	Conductivity (W/m·K)	Density (kg/m³)
Soil	2000	1.15	1300

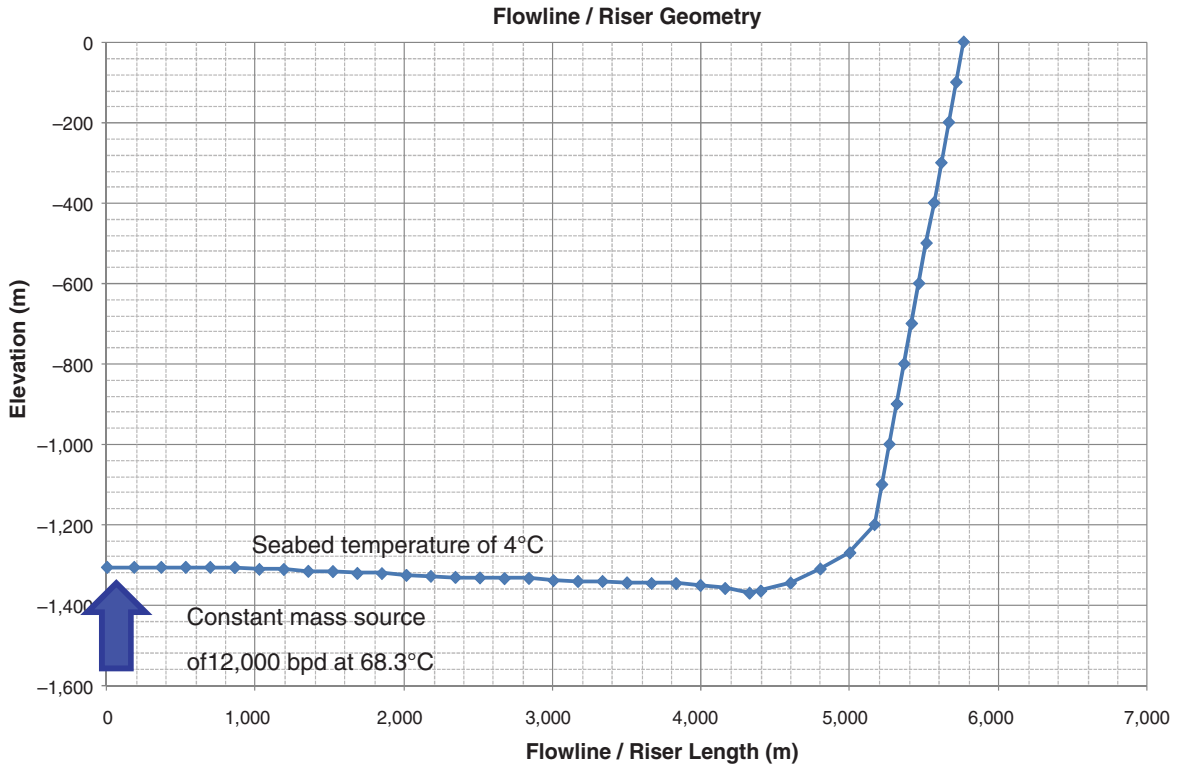

Fig. 9—Schematic of flowline and riser along with the production source (i.e., the well).

(Pedersen et al. 1992) are used to calculate the critical properties and acentric factor of pseudocomponents. Pseudocomponent critical properties are varied to match the calculated bubblepoint to that obtained from the laboratory measurement using a recombination of separator samples at the reservoir temperature.

The wax phase envelope is calculated using *n*-paraffin distribution from HTGC measured values presented in Table 6. The match between experimental and calculated WATs is obtained by varying the solid-phase activity coefficient correction factor. Hydrate equilibrium phase behavior calculations are calculated using the composition of the recombination fluid drawn down to the line condition. Because there were no hydrate measurements, we relied on simulation results, as presented in **Fig. 10.** All thermodynamic modeling results, pressure/temperature phase boundaries for vapor/liquid equilibria, and wax and hydrate loci are presented in Fig. 10. In Fig. 10, we also illustrate the pressure and temperature conditions at reservoir, wellhead, and at the floating productivity, storage, and offloading (FPSO) arrival. As seen in Fig 10, production profile from reservoir P/T, to wellhead P/T, to FPSO-arrival P/T does not intersect any of the phase boundaries. Hence, it is not expected to cause any issues with wax and hydrate precipitation and deposition.

Fluid Rheological Behavior. The non-Newtonian flow associated with gels is modeled using the Bingham plastic model (Bingham 1922; Darby and Melson 1981), which requires two parameters: plastic viscosity (PV) and GS. The PV is the slope of the shear-stress-vs.-shear-rate line after the gel is broken. PV represents the viscosity of a fluid when extrapolated to infinite shear rate on the basis of Bingham-model mathematics. The PV for STO and reservoir fluid at line-pressure conditions has been determined using the rheometer data presented earlier in Figs. 7 and 8 at a line temperature of 40°C and at subsea temperature of 4°C. In Figs. 7 and 8, the viscosity data are presented as a function of shear rate. The shear-stress-vs.-shear-rate data are then regressed to obtain PV, as presented in **Fig. 11.** As seen in Fig. 11, a linear equation is derived from the gradient of shear stress vs. shear rate. The respective gradients for STO and fluid at line pressure condition with solution gas are 0.0504 Pa·s (50.4 cp) and 0.0322 Pa·s (32.2 cp), respectively. The laboratory measured GS is then directly used in the Bingham plastic model as the intercept.

Modeling of Flowline Shutdown and Cooling Profile. The protocol followed to assess the potential of gelling associated with the unplanned shutdown for the present study is listed below:

1. Steady-state flow condition is first established in the flowline/riser system using the OLGA multiphase simulation software for the following two cases:
   a. One with the Bingham non-Newtonian parameters based on stock-tank pressure (i.e., the flowline depressurized from a line pressure of 2,200 psi to release the dissolved gas after the line is shut down).
   b. The second model is with the Bingham non-Newtonian parameters based on a line pressure of 2,200 psia.
2. Each system is then shut down simultaneously at the wellhead and topside valves over a period of 5 minutes. The system is then allowed to cool down until an average fluid temperature of 4°C is achieved.
3. Consequently, each stabilized system is subjected to restart using two ramp-up plans. In these simulations, the topside valve is assumed to open over a 5-minute period. The two ramp-up scenarios are

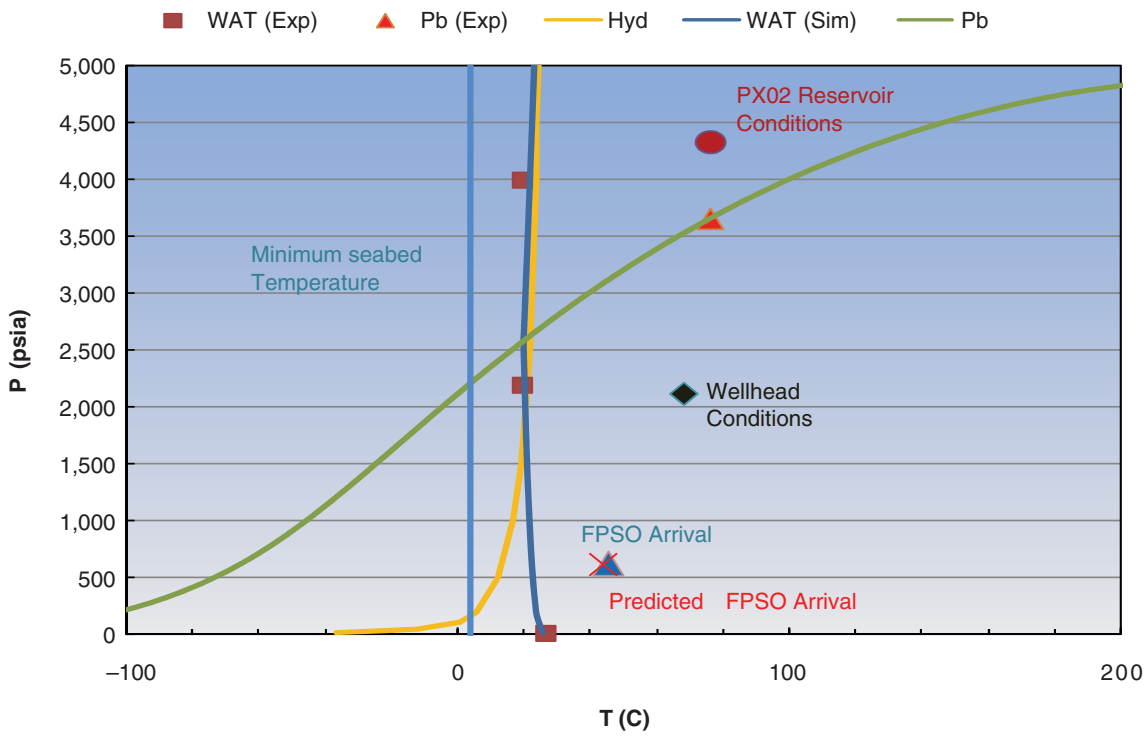

Fig. 10—Combined phase boundaries along with pressure and temperature conditions at various nodes in the production circuit.

a. A fast 6,000-B/D wellhead ramp up to 12,000-B/D total flow (i.e., 2-hour ramp up).

b. A slower 2,000-B/D wellhead ramp up to 12,000-B/D total flow (i.e., 6-hour ramp up).

The liquid-holdup scenario is presented in **Fig. 12.** Two distinct zones of 100% liquid are illustrated in Fig. 12. With sufficient cooling time, the liquid slug is expected to turn completely into gel. These liquid slugs occur at approximately 1400 to 2800 m and 3000 to 5200 m from the wellhead. This means that at the restart, the incoming fluid must effectively compress the vapor space before shearing the gelled fluid. Hence, the frequently used analytical equation (Eq. 1) to estimate shear pressure required for breakthrough based only on total gelled length is likely to be unrealistic.

However, as seen in Fig. 12, at 1.4 hours the gelled liquid is virtually in one continuous zone, and is ready to shear completely. At 1.5 hours, the gelled fluid has moved, and there are no areas of 100% liquid holdup in the flowline/riser. This effect is similar for fluid at line condition with solution gas and for stock-tank fluid.

Fig. 13 illustrates the simulated temperature and pressure curves for the STO case at three nodes including the inlet to the flowline, the base of the riser, and the top of the riser when both the wellhead and topside valves are shut down and the system is allowed to cool to ambient temperature. Fig. 13 illustrates that the fluid in the submerged flowline/riser sections cools down to approximately 5°C within 3 days of shut-in. Consequently, it takes another 2 days to reach the ambient seabed water temperature of

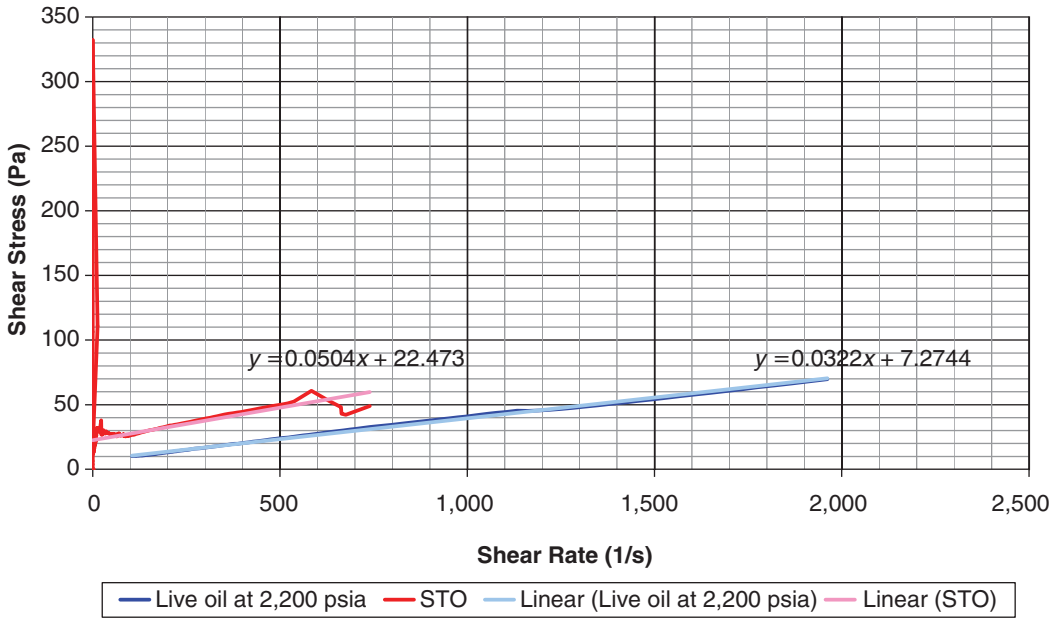

Fig. 11—Shear-stress-vs.-shear-rate data for STO at 4°C.

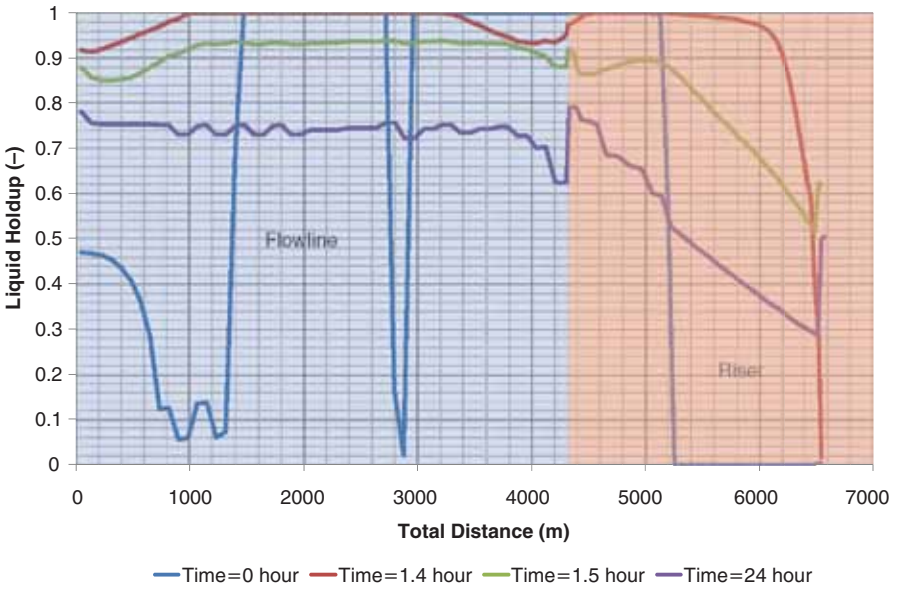

Fig. 12—Liquid holdup in the flowline during shutdown.

4°C. Pressure initially rises at the riser topside; this occurs because of the movement of gas up the riser.

The WAT of STO is measured to be 27°C. As can be seen in Fig. 13, the cooling flowline temperature would reach WAT in 18 hours at the riser base and start to form wax particles.

Similarly, the temperature and pressure profiles at three nodes including the inlet to the flowline, the base of the riser, and at the top of the riser are identical to the case when line pressure is maintained at 2,200 psia when both the wellhead and topside valves are shut in over 5 minutes and the system is allowed to cool to ambient temperature. The WAT for the reservoir fluid at 2,200 psia with solution gas is measured to be 20°C, so the riser base is expected to form wax particles after 24 hours, as opposed to 18 hours for the case of STO conditions.

Modeling of Flowline Restart. ***Stock-Tank-Condition Case.*** After attaining the gelling condition, a fast restart scenario is simulated by opening the wellhead choke at 6,000 B/D up to a rate of 12,000 B/D (in 2 hours) and the topside valve is opened in 5 minutes. Example temperature and pressure curves are illustrated in **Fig. 14** for the fast restart (2 hours). As seen in Fig. 14, a maximum pressure of 2,506 psia is required at the inlet of the flowline at approximately 1.5 hours after restart has begun to restart the flow successfully for the STO case. At this time, the temperature falls at the riser topside, which is consistent with the commencement of flow [i.e., the Joule-Thomson (J-T) effect]. Similarly, a slow-restart scenario is simulated using 2,000 B/D for the STO case to a full-flow condition of 12,000 B/D (in 6 hours). In this case also, the wellhead flow is restarted over 6 hours and the topside valve is opened over 5 minutes. For this case, a maximum pressure of 2,562 psia is required at the inlet of the flowline at approximately 2.25 hours after restart has begun in order to restart flow successfully.

Reservoir Fluid at Line-Pressure Condition of 2,200 psi With Solution-Gas Case. Similar to the STO case, the restart is simulated at two startup rates: 2,000 B/D and 6,000 B/D. **Fig. 15** illustrates the temperature and pressure curves for reservoir fluid at line-pressure conditions at the inlet to the flowline, the base of the riser, and at the top of the riser for a fast restart (2 hours). The wellhead flow is restarted over 2 hours, and the topside valve is opened over 5 minutes. To break the gel for the case in which solu-

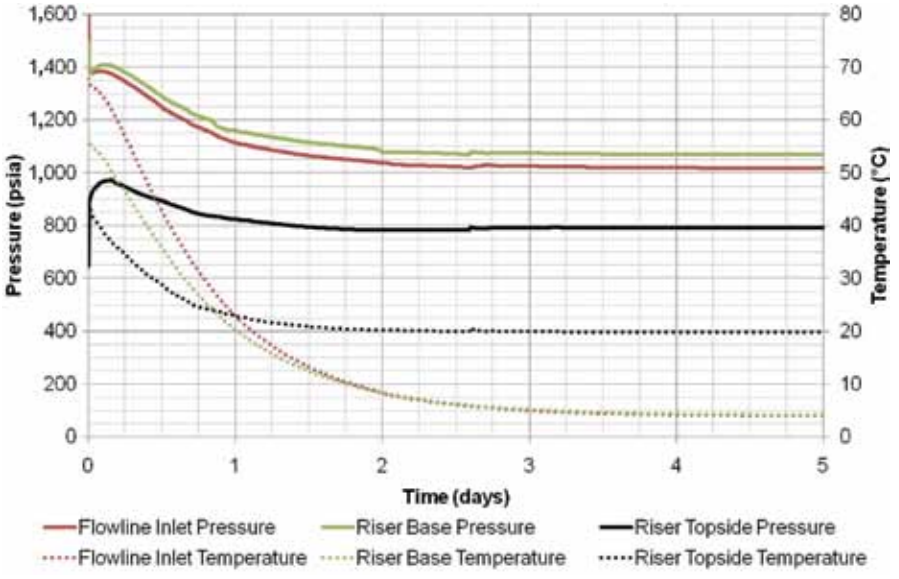

Fig. 13—Shut-in pressures and temperatures at key nodes in the flow system for STO conditions.

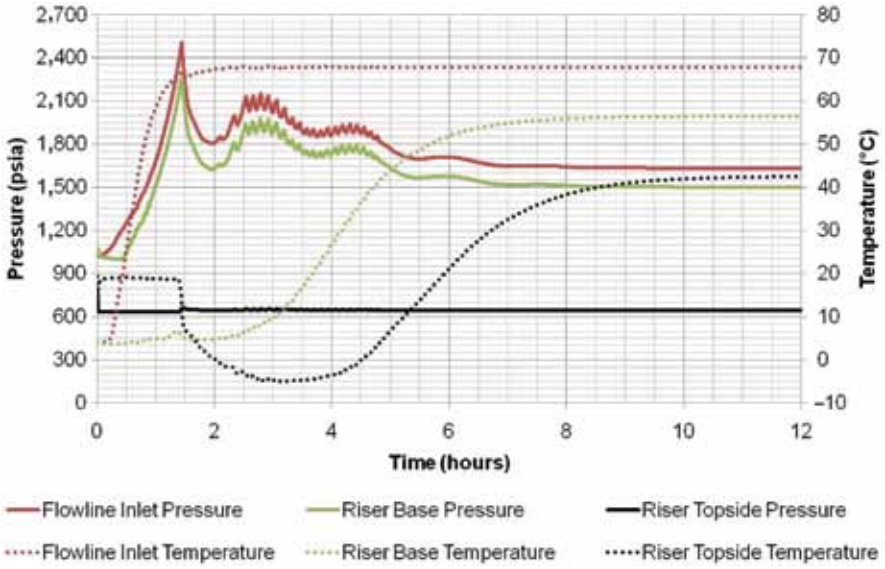

Fig. 14—Temperature and pressure profiles at key nodes for 6,000-B/D restart for STO.

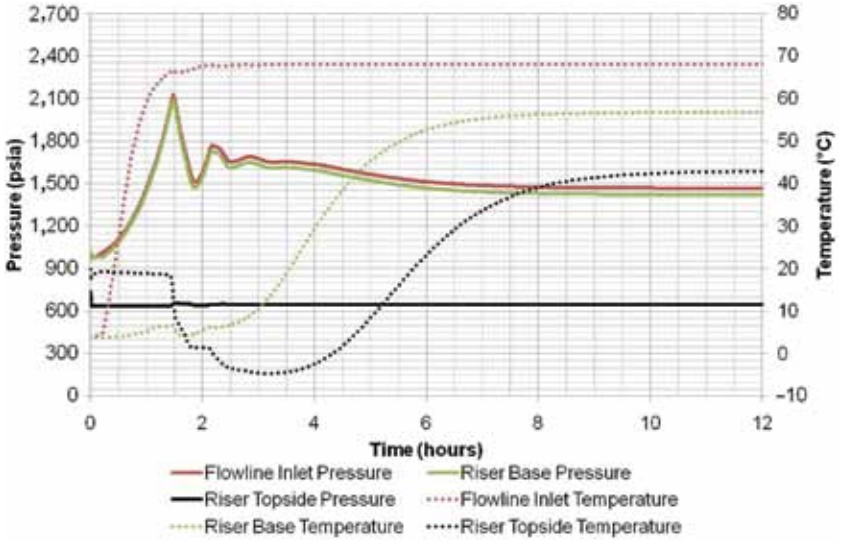

Fig. 15—Temperature and pressure profiles at key nodes for 6,000-B/D restart for fluid kept at line pressure.

tion gas is maintained in the fluid, a maximum pressure of 2,124 psia is required at the inlet of the flowline at approximately 1.5 hours after the restart (Fig. 15). At this time, the temperature falls at the riser topside, which is consistent with the commencement of flow (i.e., the J-T effect). Similar to STO, with the slow restart (6 hours), a maximum pressure of 2,142 psia is required at the inlet of the flowline at approximately 2.25 hours.

Discussion

All restart pressure conditions are presented in **Table 10.** As seen in Table 3, the fast and slow restarts did not have a significant difference in wellhead-pressure requirements to restart the flowline. However, because of dissolved gas in the line, the flowline restart pressure requirement was approximately 400 psi lower than that of the STO case. This is because of the gas-dissolution effect lowering the viscosity and also the GS of the liquid in the flowline. Also, experimental findings dictate that the gel is not expected to form using a 300 ppm concentration of PPD.

The field measurement shows that the current flowing wellhead pressure is approximately 2,200 psi and the shut-in wellhead pressure is 2,600 psi. Both these pressures are higher than the simulated restart pressure. Hence, in the case of prolonged unplanned shutdown of the flowline, the fluid is expected to form a gel and the current wellhead pressures are adequate to break the gel and regain the flow.

TABLE 10—SUMMARY OF RESTART PRESSURES

	STO conditions		Line-pressure conditions	
	Fast restart	Slow restart	Fast restart	Slow restart
	(2 hours)	(6 hours)	(2 hours)	(6 hours)
Restart pressure (psi)	2,505	2,562	2,124	2,142

Conclusions

- As expected, solution gas at line conditions provided lower WAT, GS, and viscosity values.
- Transient simulation of shutdown scenarios with experimental validation and the appropriate viscosity model provided longer shut-in time (24 hours) to reach WAT of 20°C at line condition as opposed to 18 hours for the STO case where WAT is 27°C.
- Continuous PPD injection provided no gelling at subsea temperature of 4°C.
- Transient simulation predicted restart pressures of approximately 2,600 psi for STO and 2,200 psi for live fluid after a prolonged shut-in period. Live-fluid pressure is smaller than the shut-in wellhead pressure. Hence, the wellhead has sufficient energy to mobilize the gel after prolonged shut-in time if the flowline is maintained at a line pressure of 2,200 psi. Therefore, there is no need for continuous PPD injection. In case the wellhead pressure decreases with time, reconsideration of the operating strategy will be in order.
- Simulated FPSO-fluid-arrival temperature and pressure conditions match quite well with the field measured values, as shown in Fig. 10.
- As an assurance, the dual flowline also has the provision of a pig-launching pump at subsea. The pig-launching pump can provide additional energy to break the gel if it forms at all.
- Waterflooding and gas-injection processes are implemented for reservoir-pressure-maintenance purposes. Therefore, the reservoir pressure is not expected to decline with time.

Acknowledgments

The authors would like to thank Murphy Oil Corporation and Schlumberger management for permission to publish this work. Also, we would like to thank the Schlumberger Marketing Communications department for their support in finalizing the manuscript.

References

Barry, G. 1971. Pumping non-Newtonian waxy crude oils. *J. Inst. Pet.* **57** (554): 76–85.

Bingham, E.C. 1922. *Fluidity and Plasticity*, Vol. 1–2. New York City: McGraw-Hill.

Darby, R. and Melson, J. 1981. How to predict the friction factors for Flow of Bingham Plastics. *Chemical Engineering* **88** (26): 56–61.

Ekweribe, C.K., Civan, F., Lee, H.S., and Singh, P. 2008. Effect of System Pressure on Restart Conditions of Subsea Pipelines. Paper SPE 115672 presented at the SPE Annual Technical Conference and Exhibition, Denver, 21–24 September. http://dx.doi.org/10.2118/115672-MS.

Karan, K., Ratulowski, J., and German, P. 2000. Measurement of Waxy Crude Properties Using Novel Laboratory Techniques. Paper SPE 62945 presented at the SPE Annual Technical Conference and Exhibition, Dallas, 1–4 October. http://dx.doi.org/10.2118/62945-MS.

Misra, S., Baruah, S., and Singh, K. 1995. Paraffin Problems in Crude Oil Production and Transportation: A Review. *SPE Prod & Oper* **10** (1): 50–54. SPE-28181-PA. http://dx.doi.org/10.2118/28181-PA.

Pedersen, K.S., Blilie, A.L., and Meisingset, K.K. 1992. PVT calculations on petroleum reservoir fluids using measured and estimated compositional data for the plus fraction. *Ind. Eng. Chem. Res.* **31** (5): 1378–1384. http://dx.doi.org/10.1021/ie00005a019.

Péneloux, A., Rauzy, E., and Fréze, R. 1982. A consistent correlation for Redlich-Kwong-Soave volumes. *Fluid Phase Equilib.* **8** (1): 7–23. http://dx.doi.org/10.1016/0378-3812(82)80002-2.

Soave, G. 1972. Equilibrium constants from a modified Redlich-Kwong equation of state. *Chem. Eng. Sci.* **27** (6): 1197–1203. http://dx.doi.org/10.1016/0009-2509(72)80096-4.

Vinay, G., Wachs, A., and Frigaard, I. 2009. Start-up of Gelled Waxy Crude Oil Pipelines: A New Analytical Relation To Predict the Restart Pressure. Paper SPE 122443 presented at the Asia Pacific Oil and Gas Conference & Exhibition, Jakarta, 4–6 August. http://dx.doi.org/10.2118/122443-MS.

Wardhaugh, L.T., Boger, D.V., and Tonner, S.P. 1988. Rheology of Waxy Crude Oils. Paper SPE 17625 presented at the International Meeting on Petroleum Engineering, Tianjin, China, 1–4 November. http://dx.doi.org/10.2118/17625-MS.

Conversion Factors

°API		141,500 / (131.5+°API)	= kg/m^3
B/D	×	1.84×10^{-6}	= m^3/s
°C		273.15 + °C	= K
psi	×	6.894757	= kPa
scf/bbl	×	0.1781071	= m^3/m^3

Sithambaram Suppiah works for Halliburton as a consulting drilling engineer. Previously, he worked at Schlumberger in MWD/LWD engineering, at Murphy Oil as a drilling and lead production engineer in deepwater exploration offshore Malaysia and well intervention and flow assurance issues. **Chris Alderson** is a production manager for Murphy Oil in Sabah, Malaysia. E-mail: Christopher_Alderson@murphyoilcorp.com. He holds a degree in mechanical engineering from Loughborough University in the UK, and an MSc degree in petroleum engineering from Heriot Watt University. Alderson has spent 22 years in the upstream oil and gas industry in field operations, technical and management positions, and has worked in Africa, Europe, the Middle East, and southeast Asia. **Kamran Akbarzadeh** is a senior research scientist and flow assurance research team leader at DBR Technology Center, Schlumberger. He has more than 11 years of research experience in flow assurance, specifically on organic solids precipitation and deposition. During Akbarzadeh's 6-year career with Schlumberger, he has managed many commercial and research projects. He holds a PhD in chemical engineering from Shiraz University in Iran. **Jinglin Gao** is currently tech services manager at Schlumberger DBR Technology Center in Edmonton, Alberta, Canada. E-mail: JGao3@exchange.slb.com. He started his career with PetroChina after graduating from Daqing Petroleum Institute in China. After 12 years working on PVT and fluid-phase behavior at PetroChina, Gao decided to pursue his higher education in Canada. He now holds an MSc degree in chemical engineering from University of Saskatchewan, Saskatoon, Saskatchewan, Canada. Gao joined DBR as a project manager in 2001, undertaking various fluid projects including PVT, EOR, and flow assurance. **James McMillan Shorthouse** is a principal flow assurance engineer for Schlumberger in Perth, Australia. He holds a BEng degree (with honors) in chemical engineering (1995) from the University of Paisley (now called University of the West of Scotland) in the UK. **Ifadat Khan** is a principal flow assurance engineer for Schlumberger in Dubai. E-mail: Ifadat@slb.com. He has 8 years of extensive experience in characterization of various flow assurance issues, assessment, and developing solutions and workflows to help customers manage flow assurance problems. Khan holds an ME degree from Indian Institute of Science, India and a PhD degree from King Fahd University of Petroleum and Minerals in Dhahran, Saudi Arabia. **Christopher Michael Forde** holds a degree from Institute of Technology Tralee in Ireland. E-mail: Chris.Forde@viking-moorings.com. His career began in all aspects of mechanical repair, process design, and implementation. Forde moved onto the mineral sector in western Australia and the Goldfield region in various supervisory roles. His career in the oilfield industry began in 2000 with Schlumberger Oilphase-DBR, where he was responsible for the set up and implementation of Schlumberger PVT Laboratories in Malaysia and Australia. Forde currently holds the position of managing director at Viking Mooring, Perth, Australia. **Abul Jamaluddin** is NExT Director of new programs and multidisciplinary courses and production domain advisor in Schlumberger. E-mail: ajamaluddin1@slb.com. He holds a BSc degree in petroleum engineering and an MSc and PhD degrees in chemical engineering. Jamaluddin has been an active member of various SPE committees including ATWs, Forum Series, and Distinguish Lecturer selection committee. He is an associate editor of SPE Prod & Oper. **Jamaluddin** chaired the IQPC Flow Assurance conference, SPE ATW on "Assuring Flow from Pore to Process" and also the forum on "Economic and Sustainability Challenges in the Future Development of Sour Gas." He was an SPE Distinguished Lecturer for the 2004–2005 season. The biography for **Afidah Ahmed** is not available.